Optimal Antenna Selection and Beamforming for an IRS Assisted System

Rimalapudi Sarvendranath, *Member, IEEE*, Ashok Kumar Reddy Chavva, *Senior Member, IEEE*, and Erik G. Larsson, *Fellow, IEEE*

***Abstract*—An intelligent reflecting surface (IRS) is a cost and energy-efficient solution to improve wireless system performance. Transmit antenna selection (AS) harnesses the benefits of multiple antennas with a smaller number of radio frequency (RF) chains. We focus on joint optimization of antenna subset and transmit beamforming at the transmitter (Tx) and passive beamforming at the IRS to maximize the receive signal power. We derive a closed-form optimal AS rule for a Tx and receiver (Rx) equipped with single RF chain each and ideal IRS. We analyze its performance with a correlated channel model and then extend it to non-ideal IRS. We also propose a simpler rule that significantly reduces the number of computations and pilots. For an Rx that performs maximal ratio combining, we propose a manifold optimization algorithm and a low-complexity selection rule. For a Tx with multiple RF chains, we propose a subset selection algorithm that yields a locally optimal solution and an alternating optimization algorithm that reduces complexity. Our simulations study the impact of estimation errors, discrete phase shifts, and channel correlation on the proposed selection rules, which perform better than the existing AS rules. They also show that the proposed low-complexity rules are near-optimal.**

***Index Terms*—Intelligent reflecting surface, antenna selection, beamforming, manifold optimization, alternating optimization, channel correlation, discrete phase shifts.**

I. Introduction

Intelligent reflecting surface (IRS) is being envisioned as a critical technology for the sixth generation (6G) wireless communication systems to achieve a smart radio environment [2], [3]. The wireless technologies based on large antenna arrays and high frequencies would need many expensive radio frequency (RF) chains, consisting of signal converters, filters, mixers, and amplifiers [4]. Instead, IRS consists of low-cost passive reflective elements such as printed dipoles [5], [6], Each of these elements can induce a programmable phase shift to the incident electromagnetic wave, which enables passive beamforming to improve the receive signal power. Hence, an IRS improves the performance of a communication system in energy and cost efficient manner.

Rimalapudi Sarvendranath is currently with the Department of Electronics and Electrical Engineering (EEE), IIT Guwahati, Guwahati, 781039, India and was with the Department of Electrical Engineering (ISY), Linköping University, 58183, Linköping, Sweden, where he did a part of the work. A. K. R. Chavva is with the Mobile Communication R & D, Samsung R & D Institute Bangalore, 560038, India and, Erik G. Larsson is with the Department of Electrical Engineering (ISY), Linköping University, 58183, Linköping, Sweden (e-mail: sarvendranath@iitg.ac.in; ashok.chavva@samsung.com; erik.g.larsson@liu.se).

The work of Rimalapudi Sarvendranath and Erik G. Larsson was sponsored in part by ELLIIT and the KAW foundation. Furthermore, the work of Rimalapudi Sarvendranath was partially sponsored by the start-up grant EEESUGIITG01354SARV001 of the IIT Guwahati.

A part of this paper was presented in IEEE WCNC, April 2021 [1].

Similar to IRS, transmit antenna selection (AS) is a technology that improves energy and cost efficiency by reducing the number of RF chains at the transmitter. In it, a transmitter selects a subset of antennas and connects them to the available RF chains, which are smaller in number than the antenna elements. AS achieves full diversity with fewer RF chains and is part of wireless standards such as Long-Term Evolution and 802.11n [4]. In addition to cost efficiency, AS reduces circuit design complexity by avoiding signal leakages and cross-talks that can occur with multiple RF chains on one integrated circuit [7]. It also reduces the amount of digital signal processing required to reduce RF impairments such as IQ imbalance and amplifier distortions [8]. Furthermore, it is shown that the performance of an IRS-assisted AS system converges to the performance of a maximal ratio transmission based system with the number of RF chains equal to the antennas at the transmitter (Tx) [9]. Motivated by this fact, we focus on addressing the challenge of pilot transmission overhead and computational complexity in an IRS-assisted AS at the Tx, which improves the performance at a low cost.

IRS-assisted systems with single and multiple antennas at the Tx are studied in the literature.

Single Input Single Output System [5], [6], [10]–[12]: An IRS is shown to improve the performance of a communication system with a single antenna transmitter and receiver (Rx) even when the direct link (Tx $\rightarrow$ Rx) between them is blocked [11], [12]. Furthermore, it achieves a diversity order equal to the number of IRS elements [10]. Symbol error probability (SEP) performance was studied in [5] and [6], and the performance of a distributed IRS system was studied in [12].

Multiple Input Single Output System With Transmit Beamforming [13]–[21]: Joint transmit beamforming at the Tx and the passive beamforming at the IRS with only reflected link (Tx $\rightarrow$ IRS $\rightarrow$ Rx) is studied in [13] and [14] and with both reflected and direct links in [15]–[20]. An alternating optimization based algorithm is developed in [15] to minimize the transmit power and different optimization algorithms were developed in [16]–[20] to maximize the receive signal power. Beamforming design for a millimeter-wave communication system is studied in [14], [16]. A fixed-point iteration method is proposed in [17] and a semi-definite relaxation (SDR) based algorithm, which yields an approximate solution, is proposed in [18]. A branch-and-bound algorithm, which converges to the global optimal solution, is presented in [20]. Furthermore, a low-complexity conjugate gradient based manifold optimization algorithm, which converges to a local-optimal solution

with near-optimal performance, is developed in [19].

Multiple Input Multiple Output (MIMO) System [22]–[24]: In [22], the complex circle manifold structure of the unit modulus constraint is exploited to jointly optimize the precoding matrices at the Tx and passive beamforming at the IRS. Two efficient algorithms were proposed to maximize the weighted sum rate of all users. A low-complexity block coordinate descent algorithm is proposed in [23] to maximize the weighted sum rate of an IRS-assisted simultaneous wireless information and power transfer system. Joint transmit and passive baemforming to minimize the SEP of an IRS-assisted MIMO system is studied in [24].

IRS With Antenna Selection [9]: A joint AS and passive beamforming algorithm is proposed in [9] for an IRS with practical reflection coefficients. In it, a single antenna with the highest channel power gain from the Tx to IRS is selected. For an IRS with a large number of elements, it is shown to achieve an optimal rate.

A. Focus and Contributions

We focus on an IRS-assisted communication system with a multiple antenna Tx communicating to a multiple antenna Rx by employing AS. We aim to develop a jointly optimal subset antenna selection, transmit beamforming at the Tx, and passive beamforming at the IRS to maximize the receive signal power. Our problem formulation is novel and practical in the following aspects. Firstly, joint AS and passive beamforming is different and involved compared to the AS in a conventional system without IRS, and the optimal AS rule is not known. Secondly, unlike [18]–[20], we do not assume any channel state information (CSI) at the IRS, which is challenging to obtain in practice due to the passive nature of the IRS. Thirdly, our approach reduces the number of pilot transmissions required. For the above model, we consider both *single AS*, where Tx is equipped with one RF chain, and *subset AS*, where Tx is equipped with more than one RF chain, scenarios.

Single AS: *1) Optimal AS Rule:* We first derive an optimal AS rule that selects the jointly optimal antenna at the Tx and the optimal reflection coefficient of each IRS element when the Rx employs Selection combining (SC). It is optimal for any number of IRS elements. For the first time, we show that the optimal antenna index and the optimal reflection coefficient are decoupled. We propose a manifold optimization local optimal AS algorithm when the Rx employs maximal ratio combining (MRC). *2) Low-Complexity AS (LAS) Rule:* We propose LAS rules for both SC and MRC. The selection metric of the LAS rule for SC lower bounds the selection metric of the optimal AS rule. These rules are robust to imperfect CSI and reduces the number of computations and pilots required. *3) Performance Analysis:* Considering the channel correlation, we analyze the performance of the optimal AS rule for SC. It handles quite involved selection metric with correlated random variables (RVs). We also derive closed-form expressions for the average signal to noise ratio (SNR) normalized by the square of the number of IRS elements and ergodic rate. These expressions provide valuable insights and apply to any number of antennas at the Tx and Rx, any number of IRS elements, and channel correlation.

Subset AS: We first develop an algorithm, which exploits the complex circle manifold structure, to find an antenna subset, transmit beamforming at the Tx, and reflection coefficients at the IRS to maximize the received signal power. It converges to a local optimal solution and its complexity grows exponentially as the number of RF chains increase. We also propose an alternating optimization based subset AS algorithm whose search complexity is independent of the number of RF chains. It inherits the advantages of the above LAS rules.

Numerical Results: Our results study the impact of different parameters on the performance of an IRS-assisted AS system. They show that the average SNR is independent of the channel correlation, whereas the diversity and the outage probability depend on the correlation. They also study the impact of discrete phase shifts and the channel estimation errors [21] on the performance of the developed AS rules. Our performance benchmarking shows that the developed optimal AS rule performs better than the AS rules in the literature and the proposed low-complexity AS rules are near-optimal.

Challenges and Comparison: Our manuscript tackles the challenges of a large number of non-convex constraints, computational complexity, and pilot transmission overhead in an IRS-assisted AS system compared to a conventional AS system. Furthermore, our analysis involves order statistics of dependent RVs, for which standard techniques employed in conventional systems without IRS are not sufficient. The single AS and subset AS algorithms developed for multiple antenna Rx differ from the single AS rule for single antenna users studied in [9]. Our AS rules only need cascaded channel gains, unlike the Tx to IRS link needed by the AS rule in [9], which is difficult to obtain for a passive IRS. Furthermore, our AS rules can compute the IRS phase shifts in parallel compared to the sequential algorithm, whose computational time increases as the number of IRS elements increase. We also note that the assumption of large number of IRS elements is used only for the asymptotic analysis.

Outline: Section II presents our system model and problem statement. The optimal single AS and LAS rules are developed in Section III. Performance analysis is done in Section IV. Section V proposes subset AS rules. Numerical results are presented in Section VI. Our conclusions follow in Section VII.

Notations: Scalars are denoted by lower-case letters. Vectors and matrices are denoted by boldface lower-case and upper-case letters, respectively. Let $j = \sqrt{-1}$. For a complex number a, $|a|$, $\arg(a)$, and a^* denote its absolute value, phase, and conjugate, respectively. The set of all complex-valued matrices of size $m \times n$ is denoted by $\mathbb{C}^{m\times n}$. For a vector vector $\mathbf{x}$, $\|\mathbf{x}\|$, $\mathbf{x}^{\mathrm{T}}$, $\mathbf{x}^{\dagger}$, and $[\mathbf{x}]_n$ denote its 2-norm, transpose, conjugate transpose, and n^{th} element, respectively. We denote the probability of an event A and the conditional probability of A given B by $\Pr(A)$ and $\Pr(A|B)$, respectively. $\mathbb{E}[\cdot]$ denotes expectation operator. For a RV X, $F_X(\cdot)$ and $f_X(\cdot)$ denote its cumulative distribution function (CDF) and probability density function (PDF), respectively. Further, $X \sim \mathcal{CN}(0, \sigma^2)$ means that X is a circular symmetric zero-mean complex Gaussian RV with variance σ^2.

II. System Model and Problem Statement

Our system model shown in Figure 1, consists of a Tx, an IRS, and an Rx. Tx has N_t antennas and $N_{RF} < N_t$ number of RF chains. It communicates to the Rx equipped with N_r antennas. IRS is equipped with N passive elements separated by d_v m and a controller that configures the reflection coefficients of the IRS elements to perform passive beamforming. The Tx dynamically selects N_{RF} antennas from the set of antennas $\{1, 2, \ldots, N_t\}$, connects them to the RF chains available, and performs transmit beamforming. It also computes the IRS reflection coefficients and sends them to the controller through a dedicated control link. The Rx either employs SC, which requires only one RF chain, or MRC, which requires N_r RF chains [25]. We assume a quasi-static flat-fading channel model [18], [19] and consider a time-division duplexing (TDD) mode of operation to exploit reciprocity.

Let $\mathbf{f}_m = [f_{m1}, \ldots, f_{mN}]^{\mathrm{T}} \in \mathbb{C}^{N\times 1}$, for $m \in \{1, 2, \ldots, N_r\}$ denote the complex baseband channel gain vector from the IRS to the m^{th} antenna of the Rx. Complex channel gain matrices from the Tx to Rx and Tx to IRS are denoted by $\mathbf{H} = [h_{mk}] \in \mathbb{C}^{N_r\times N_t}$ and $\mathbf{G} = [g_{nk}] \in \mathbb{C}^{N\times N_t}$, respectively. The channel gains from k^{th} antenna of the Tx to different IRS elements are correlated due to the rectangular geometry and size of the IRS element [26]. Similarly, channel gains from the IRS to the Rx are correlated. However, we assume that the direct link channel gains from Tx to Rx, channel gains from the Tx to IRS and IRS to Rx corresponding to different antennas at the Tx and Rx are independent. This is possible when the Tx and Rx antennas are sufficiently spaced [27], [28].

Let $r \in \{1, 2, \ldots, N_r\}$ denote the antenna selected at the Rx when it employs SC. Set S, which is a subset of $\{1, 2, \ldots, N_t\}$, contains the indices of the selected N_{RF} antennas. Let $\mathcal{S}$ denote the set of all such possible subsets containing $\binom{N_t}{N_{RF}}$ elements. Let $\mathbf{h}_{mS} \in \mathbb{C}^{N_{RF}\times 1}$ denote the channel gain vector from the Tx to m^{th} Rx antenna corresponding to the subset S and $\mathbf{G}_S \in \mathbb{C}^{N\times N_{RF}}$ denote the sub-matrix that contains columns of $\mathbf{G}$ corresponding to the antenna indices in S. Let $x_n = \beta_n e^{j\theta_n}$ denote the reflection coefficient of the n^{th} IRS element, where $\beta_n \in [0, 1]$ and $\theta_n \in [0, 2\pi]$ denote its amplitude and phase coefficients. Let $\mathbf{x} = [x_1, \ldots, x_N]^{\mathrm{T}}$ be the passive beamforming vector at the IRS. The Tx selects a subset of antennas in S, employs a transmit beamforming vector $\mathbf{w} = [w_k] \in \mathbb{C}^{N_{RF}\times 1}$, and transmits a data symbol d ($\mathbb{E}\left[|d|^2\right] = 1$). Then the m^{th} Rx antenna receives $\mathbf{h}_{mS}^{\mathrm{T}}\mathbf{w}d$ in the direct link and $\sum_{n=1}^{N} f_{mn}x_n \left[\mathbf{G}_S\mathbf{w}\right]_n d$, where $\left[\mathbf{G}_S\mathbf{w}\right]_n$ denotes the n^{th} element of the vector $\mathbf{G}_S\mathbf{w}$, in the reflected link. The combined signal y_m is given by

$$y_m = (\mathbf{h}_{mS}^{\mathrm{T}} + \mathbf{x}^{\mathrm{T}}\mathbf{F}_m\mathbf{G}_S)\mathbf{w}d + z, \tag{1}$$

where $\mathbf{F}_m = \mathrm{diag}\left(\mathbf{f}_m\right)$ and $z \sim \mathcal{CN}\left(0, \sigma_n^2\right)$ denote the additive white Gaussian noise.

A. CSI Acquisition Procedure and Assumptions [29], [30]:

The Rx sends pilot symbols and the Tx estimates the CSI in two phases. In the first phase, all the IRS elements are set to absorption mode, i.e., $\beta_n = 0$, and Tx estimates direct link channel gains. In the second phase, the IRS elements are configured to reflect mode, i.e., $\beta_n \neq 0$, and the Tx estimates the sum of the direct link and reflected link channel gains [29], [30]. Then, the Tx subtracts the direct link channel gain to get the cascaded reflected link channel gain. Individual channel gains of the Tx to IRS and the IRS to Rx links, which are challenging to obtain due to the passive nature of the IRS, are not needed at the Tx. Furthermore, no CSI is assumed at the IRS. The Tx sends the index of the Rx antenna selected and a pilot in the downlink transmission. The Rx exploits this to estimate the effective channel gain corresponding to the antennas selected and passive beamforming vector $\mathbf{x}$ programmed at the IRS.

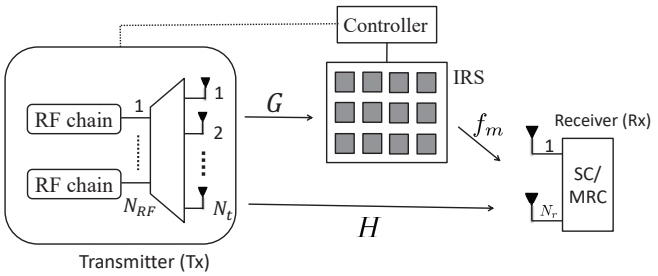

Fig. 1. System model consists of a Tx equipped with N_t antennas and N_{RF} RF chains communicating to a multiple antenna Rx with the help of an N element IRS.

B. Problem Statement

We now state our problem formally. Let ϕ denote the set of variables to be jointly optimized. When Rx employs SC $\phi = \{S, \mathbf{w}, \mathbf{x}, r\}$ and for MRC $\phi = \{S, \mathbf{w}, \mathbf{x}\}$. From (1), the instantaneous SNR γ at the Rx, when it employs SC is given by

$$\gamma = \mathsf{SNR}\left(\phi\right) = \left|(\mathbf{h}_{rS}^{\mathrm{T}} + \mathbf{x}^{\mathrm{T}}\mathbf{F}_r\mathbf{G}_S)\mathbf{w}\right|^2/\sigma_n^2. \tag{2}$$

and similarly, for MRC, it is given by

$$\gamma = \mathsf{SNR}\left(\phi\right) = \sum_{m=1}^{N_r} \left|(\mathbf{h}_{mS}^{\mathrm{T}} + \mathbf{x}^{\mathrm{T}}\mathbf{F}_m\mathbf{G}_S)\mathbf{w}\right|^2/\sigma_n^2. \tag{3}$$

Let $\mathsf{R}\left(\phi\right) = \log_2\left(1 + \mathsf{SNR}\left(\phi\right)\right)$ denote the instantaneous rate. Similarly, the instantaneous SEP $\mathsf{SEP}\left(\phi\right)$ is given by [31, eq. (14)]

$$\mathsf{SEP}\left(\phi\right) \approx c_1 \exp\left(-c_2\mathsf{SNR}\left(\phi\right)\right). \tag{4}$$

Our objective is to maximize received signal power at the receiver, which maximizes instantaneous rate and minimizes instantaneous SEP, subject to the following two constraints:

1) *Peak transmit power constraint* limits the instantaneous transmit power to be below a maximum transmit power $P_{\max}$ allowed, i.e., $\|\mathbf{w}\|^2 \leq P_{\max}$ [18].
2) *Unit modulus constraint* limits the modulus of each IRS reflection coefficient to be one i.e., $|x_n| = 1$, for $n \in \{1, 2, \ldots, N\}$ [14], [15], [19], [20].

Problem: Our optimization is over $\phi = \{S, \mathbf{w}, \mathbf{x}, r\}$, for SC and $\phi = \{S, \mathbf{w}, \mathbf{x}\}$, for MRC, which can be written as

$$\mathcal{P}: \quad \max_{\phi} \quad \mathsf{SNR}(\phi), \tag{5}$$

$$\text{s.t.} \quad \|\mathbf{w}\|^2 \leq P_{\max}, \tag{6}$$

$$|x_n| = 1, \ \forall \ n = 1, \ldots, N. \tag{7}$$

The above optimization problem $\mathcal{P}$ is non-convex as the objective function is non-concave and the unit-modulus constraint is non-convex. To the best of our knowledge, there is no simple tractable solution to this problem.

III. Single Antenna Selection With IRS ($N_{RF} = 1$)

In this section, for SC, we first derive an optimal solution of $\mathcal{P}$ for ideal reflection coefficients and then adapt it to non-ideal coefficients. We also propose a LAS rule and a two pilot power scheme to reduce the complexity and pilot power consumption. Then for MRC, we develop an optimal selection algorithm and a LAS rule.

A. Selection Combining

Let $s \in \{1, 2, \ldots, N_t\}$ and $r \in \{1, 2, \ldots, N_r\}$ denote the indices of the antennas selected at the Tx and Rx, respectively, and w_s denote the corresponding element in the beamforming vector $\mathbf{w}$. Here, the received signal in (1) and the instantaneous SNR in (2) reduces to

$$y_r = \left(h_{rs} + \sum_{n=1}^{N} f_{rn} g_{ns} x_n \right) w_s d + z, \tag{8}$$

and

$$\gamma = \mathsf{SNR}(s, w_s, \mathbf{x}, r) = \left| h_{rs} + \sum_{n=1}^{N} f_{rn} g_{ns} x_n \right|^2 \frac{|w_s|^2}{\sigma_n^2}, \tag{9}$$

respectively.

1) Optimal AS Rule for Ideal IRS Coefficients: We first present the optimal AS rule for ideal reflection coefficients.

Result *1:* For an IRS-assisted single AS, the optimal Tx antenna s_{opt}, optimal transmit power $w_{s_{\text{opt}}}^2$, optimal Rx antenna r_{opt}, and optimal reflection coefficient $x_{n,\text{opt}}$ are given by $w_{s_{\text{opt}}}^2 = P_{\max}$,

$$(r_{\text{opt}}, s_{\text{opt}}) = \underset{\substack{m \in \{1,2,\ldots,N_r\}, \\ k \in \{1,2,\ldots,N_t\}}}{\arg\max} \left\{ |h_{mk}| + \sum_{n=1}^{N} |f_{mn} g_{nk}| \right\}, \tag{10}$$

$$x_{n,\text{opt}} = \exp\left(j \left[\arg\left(h_{r_{\text{opt}} s_{\text{opt}}} \right) - \arg\left(f_{r_{\text{opt}} n} g_{n s_{\text{opt}}} \right) \right] \right), \tag{11}$$

for $n \in \{1, 2, \ldots, N\}$.

Proof: The proof is given in Appendix A. ∎

Insights: From (10), we see that the optimal antenna pair is the one that maximizes the selection metric, which is the sum of the absolute values of the direct link and the N cascaded reflected link channel gains. The optimal phase of each IRS element is the difference between the direct link phase and the reflected link phase. We see that the optimal antenna indices depend only on the absolute values of the channel gains and the optimal reflection coefficients depend only on their phases. They are also decoupled, allowing us to directly find the optimal antenna indices.

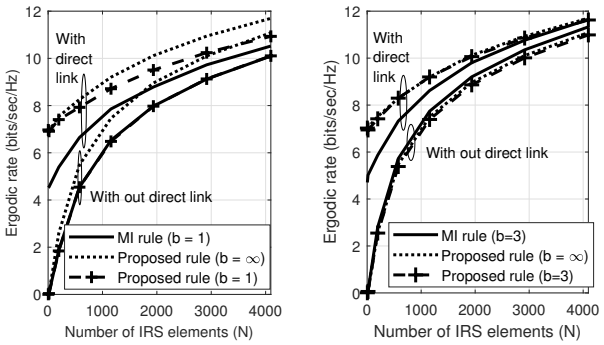

(a) $b = 1$ (b) $b = 3$

Fig. 2. Performance comparison: Ergodic rate as a function of the number of IRS elements with non-ideal gain ($P_{\max} = 10$ dBm, $N_t = 16$, $N_r = 1$, $N_{RF} = 1$, $d_v = \lambda/2$ $d_{ti} = 40$ m, $d_{tr} = 20$ m).

Number of Pilot Transmissions Required and Computational Complexity: Here, the Tx and Rx have only one RF chain each, which they switch to each antenna, to estimate the channel gains at the Tx. Hence, the Rx needs to transmit $N_t N_r$ pilots in the first phase to estimate direct link channel gains and $N_t N_r N$ pilots in the second phase to estimate reflected link channel gains. In total, we need $N_t N_r + N_t N_r N$ pilots. Furthermore, we need $\mathcal{O}(N_t N_r N)$ computations to select optimal antennas and compute optimal reflection coefficients.

2) AS Rule for Non-Ideal IRS Coefficients: In this section, we consider non-ideal IRS Coefficients, where θ_n can only take discrete values and the amplitude coefficient β_n depends on the phase configured. Let b denote the number of bits used to denote the 2^b discrete values that θ_n can take. The phase dependent amplitude coefficient $\beta_n(\theta_n)$ is as follows [9, (6)]

$$\beta_n(\theta_n) = 0.2 + 0.8 \left(\frac{1 - \sin(\theta_n - 0.43\pi)}{2} \right)^{1.6}, \ \theta_n \in [0, 2\pi]. \tag{12}$$

We now adapt the optimal AS rule in Result 1 to the above non-ideal IRS coefficients. Here, antennas are selected as per (10) and discrete value of θ_n is obtained by quantization, i.e.,

$$\theta_n = \text{quant}\left(\arg\left(h_{r_{\text{opt}} s_{\text{opt}}} \right) - \arg\left(h_{r,n} g_{n s_{\text{opt}}} \right) \right), \tag{13}$$

where quant $(\cdot)$ denotes uniform quantization operation.

We now compare the performance of this proposed practical AS rule with the AS rule in [9] that is designed for non-ideal IRS coefficients. We shall refer to it as maximum IRS (MI) rule as it selects the antenna s_{mi} with maximum channel power from the Tx to IRS, i.e., $s_{\text{mi}} = \arg\max_{k \in \{1,2,\ldots,N_t\}} \{\|\mathbf{g_k}\|\}$, where $\mathbf{g_k} \in \mathbb{C}^{N \times 1}$ is the k^{th} column of the Tx to IRS channel matrix $\mathbf{G}$. Discrete phase of each IRS element is obtained sequentially using Algorithm 1 in [9].

Figure 2 plots the ergodic rate as a function of the number of IRS elements for the MI rule and proposed AS rule with non-ideal IRS coefficients. Comparison is made for two

scenarios; i) with a direct link and ii) without direct link.[1] Figures 2a and 2b does this for $b = 1$ and $b = 3$, respectively. *i)* $b = 1$*:* Without direct link, the performance of the proposed rule matches with the MI rule. However, with direct link, the proposed rule performs better than the MI rule for all values of N. *ii)* $b = 3$*:* Without direct link, the proposed rule is close to the MI rule for small N, and the MI rule performs slightly better for large N. With a direct link, the proposed rule performs significantly better than the MI rule for small N and matches with the MI rule for large N. Furthermore, the performance with $b = 3$ matches with the continuous phase.

Benefits of the Proposed Rule: From the above, we see that the proposed practical AS rule performs well even with non-ideal IRS coefficients. Moreover, it can compute the discrete phase shits in parallel compared to sequential computation in the MI rule, which increases the computation time as N increases. Given these benefits, in subsequent sections, we assume ideal IRS coefficients and focus on developing AS rules that require lower number of pilot transmissions.

3) LAS Rule: We now propose a simpler LAS rule and a two pilot power CSI acquisition procedure. For Rx antenna m and Tx antenna k, it computes the selection metric $|h_{mk}| + \left|\sum_{n=1}^{N} f_{mn} g_{nk}\right|$ and selects the antenna combination (r, s) that maximizes it. Once the antennas are selected, the corresponding reflection coefficient x_n is computed by substituting the phases of the direct link h_{rs} and reflected link channel gain $f_{rn} g_{ns}$ as in (11). Therefore, the LAS rule is given by

$$(r, s) = \underset{\substack{m \in \{1,2,\ldots,N_r\}, \\ k \in \{1,2,\ldots,N_t\}}}{\arg\max} \left\{ |h_{mk}| + \left| \sum_{n=1}^{N} f_{mn} g_{nk} \right| \right\}, \tag{14}$$

$$x_n = \exp\left(j \left[\arg\left(h_{rs}\right) - \arg\left(f_{rn} g_{ns}\right)\right]\right), \ \forall \ n, \tag{15}$$

and $w_s^2 = P_{\max}$. By the triangle inequality, we know that

$$\left| \sum_{n=1}^{N} f_{mn} g_{nk} \right| \leq \sum_{n=1}^{N} \left| f_{mn} g_{nk} \right|. \tag{16}$$

Therefore, the selection metric of the LAS rule lower bounds the selection metric of the optimal AS rule in (10).

We now propose a two pilot power CSI acquisition scheme for the LAS rule. *i) Low Pilot Power Phase:* First, with IRS in absorption mode, the Rx transmits $N_t N_r$ pilots with pilot power P_1 to obtain the estimates of $|h_{11}|, \ldots, |h_{N_r N_t}|$. Following that the IRS is set to reflective mode with $x_n = 1, \ \forall \ n$. Then Rx sends another $N_t N_r$ pilots to obtain the estimates of absolutes of sum of cascaded channel gains, i.e., $\left|\sum_{n=1}^{N} f_{1n} g_{n1}\right|, \ldots, \left|\sum_{n=1}^{N} f_{N_r n} g_{n N_t}\right|$. Now the Tx selects the antenna combination (r, s) as per (14) using this CSI obtained with low pilot power. Then, it connects the RF chain to the antenna index s and communicates the antenna index r to Rx. *ii) High Pilot Power Phase:* Then, the Rx sends $N + 1$ pilots with power $P_2 \geq P_1$ to obtain estimates of $\arg(h_{rs}), \arg(f_{r1} g_{1s}), \ldots, \arg(f_{rN} g_{Ns})$ required to compute x_n in (15). Therefore, the LAS rule needs only $2N_t N_r + N + 1$ pilots compared to $N_t N_r + N_t N_r N$ pilots required by the optimal AS rule. and its computational complexity is $\mathcal{O}(N_t N_r + N)$. Thus, the LAS rule combined with the two pilot power scheme reduces the pilot power consumption and number of pilots and the computations required significantly.

The motivation behind using lower power to obtain amplitudes of channel gains and higher power to obtain their phases is from the fact that the phase information is crucial to ensure coherent reception. In Section VI, we see that this procedure saves pilot power with only a minor performance degradation.

B. MRC

Here, the Rx is equipped with N_r RF chains. For antenna s selected at the Tx, the instantaneous SNR in (3) reduces to

$$\gamma = \mathsf{SNR}\left(s, P_{\max}, \mathbf{x}\right) = \frac{P_{\max}}{\sigma_n^2} \sum_{m=1}^{N_r} \left| h_{ms} + \sum_{n=1}^{N} f_{mn} g_{ns} x_n \right|^2. \tag{17}$$

Let $\mathbf{x}_k = [x_{nk}] \in \mathbb{C}^{N \times 1}$ denote the passive beamforming vector configured when Tx antenna k is used for transmission. For any Tx antenna k, $\mathbf{x}_k$ that maximizes the signal power can be obtained by solving:

$$\mathcal{P}_k: \quad \max_{\mathbf{x}_k} \quad \sum_{m=1}^{N_r} \left| h_{mk} + \sum_{n=1}^{N} f_{mn} g_{nk} x_{nk} \right|^2, \tag{18}$$

$$\text{s.t.} \quad |x_{nk}| = 1, \quad n = 1, \ldots, N. \tag{19}$$

The objective function in $\mathcal{P}_k$ is quadratic in $\mathbf{x}_k$ and is convex. However, the unit modulus constraint is non-convex and standard convex optimization techniques cannot be employed.

We now first define *manifold* and then present an optimization technique that can be used to solve $\mathcal{P}_k$. A manifold is a topological space that looks like a Euclidean space in the vicinity of each point.[2] The constraint $|x_{nk}| = 1$ forms a circle in a complex plane. Hence, the unit modulus constraint in (19) is a product of N complex circles, which forms a complex circle manifold. It is a Riemannian submanifold of $\mathbb{C}^{N \times 1}$ [19], [22], for which we can find a vector that gives direction in which the objective function increases similar to a gradient in the Euclidean space. This is referred to as Riemannian gradient. For a complex circle manifold, this is given by the orthogonal projection of the Euclidean gradient onto the tangent space at that point. Geometric interpretation of these gradients is shown in [22, Fig. 2]. Using this Riemannian gradient, the optimization techniques developed for the Euclidean space can be modified to solve $\mathcal{P}_k$ [32]. These techniques converge to the local optimal solution [22].

1) The Optimal AS Rule for MRC: The optimal selection algorithm when Rx employs MRC is as follows:

Step 1: For each $k \in \{1, 2, \ldots, N_t\}$, solve $\mathcal{P}_k$ using conjugate gradient based manifold optimization technique to obtain $\mathbf{x}_k^{\text{opt}}$.

Step 2: Then select the Tx antenna that maximizes the SNR, i.e.,

$$s_{\text{opt}} = \underset{k \in \{1,2,\ldots,N_t\}}{\arg\max} \left\{ \mathsf{SNR}\left(k, P_{\max}, \mathbf{x}_k^{\text{opt}}\right) \right\}, \tag{20}$$

[1]The MI rule is originally developed for the case when there is no direct link. For a fair comparison, we updated its phase selection algorithm to align the received signal in the direction of the direct link.

[2]A more formal definition can be found in [32].

and configure $\mathbf{x}_{s_{\text{opt}}}^{\text{opt}}$ as IRS reflection coefficients.

Here, we see that the optimal antenna indices and the reflection coefficient are no longer decoupled. Similar to optimal AS rule in Result 1, we need $N_tN_r + N_tN_rN$ pilots For each antenna k, the above algorithm uses the conjugate gradient based manifold optimization technique to solve $\mathcal{P}_k$, whose worst-case complexity is $\mathcal{O}(N^{1.5})$ [19]. Therefore, the computational complexity of the above algorithm is $\mathcal{O}(N_tN^{1.5})$.

2) LAS Rule for MRC: The objective function of $\mathcal{P}_k$ in (18) is sum of the absolute squares of the effective channel gains. To reduce the computational complexity involved in maximizing it, we consider an objective function, which is sum of absolutes, i.e., $\sum_{m=1}^{N_r}\left|h_{mk}+\sum_{n=1}^{N} f_{mn}g_{nk}x_{nk}\right|$. By triangle inequality, it is lower bounded by $\left|\sum_{m=1}^{N_r} h_{mk}+\sum_{n=1}^{N} x_{nk}\sum_{m=1}^{N_r} f_{mn}g_{nk}\right|$.

Let $a_k = \sum_{m=1}^{N_r} h_{mk}$ and $b_{nk} = \sum_{m=1}^{N_r} f_{mn}g_{nk}$. Therefore, the lower bound reduces to $\left|a_k+\sum_{n=1}^{N} x_{nk}b_{nk}\right|$. The reflection coefficient that maximizes this lower bound can be computed similar to (15). It is given by $x_{nk} = \exp\left(j\left[\arg\left(a_k\right)-\arg\left(b_{nk}\right)\right]\right),\ \forall n$. Substituting this in the lower bound, it reduces to $|a_k|+\sum_{n=1}^{N}|b_{nk}|$. Using these, we propose the following LAS rule for MRC:

$$s = \underset{k\in\{1,2,\ldots,N_t\}}{\arg\max}\left\{|a_k|+\sum_{n=1}^{N}|b_{nk}|\right\}, \tag{21}$$

$$x_{ns} = \exp\left(j\left[\arg\left(a_s\right)-\arg\left(b_{ns}\right)\right]\right),\ n=1,\ldots,N. \tag{22}$$

Here, the antenna index and the reflection coefficient are decoupled different from the optimal rule. The above LAS rule needs only channel gains summed over N_r receive antennas. Therefore, we only need $N_t + N_tN$ pilots compared to the $N_tN_r+N_tN_rN$ pilots required by the manifold based optimal rule. Furthermore, computational complexity is $\mathcal{O}(N_tN)$. In the lines similar to the development of the LAS rule in Section III-A3 the selection metric in (21) can be modified to $|a_k| + \left|\sum_{n=1}^{N} b_{nk}\right|$. This will further reduce the pilot transmissions to $2N_t + N$. We can also utilize the two pilot power scheme described in Section III-A3 to further reduce the pilot power.

IV. Performance Analysis of the Optimal AS Rule

In this section, we analyze the performance of the optimal single AS rule in Result 1. With correlated channel model, we first derive expressions for the average SNR, outage probability, ergodic rate, and average SEP, which needs to be evaluated numerically. We then derive a closed-form expressions for the normalized average SNR and approximate ergodic rate.

We consider the channel gains from the Tx to IRS and the IRS to Rx to undergo correlated Rician fading. This models the scenarios where IRS is located such that there is a line of sight (LOS) path from itself to the Tx and the Rx. Let K_g, $\mathbf{G}^{\text{LOS}}$, and $\mathbf{G}^{\text{NLOS}}$ denote the Rician factor, LOS, and non-LOS (NLOS) components, respectively, of the Tx to IRS link and K_r, $\mathbf{f}_m^{\text{LOS}}$, and $\mathbf{f}_m^{\text{NLOS}}$ denote the Rician factor, LOS, and NLOS components, respectively, of the IRS to Rx link. Let μ_g and μ_r denote the average channel power gains of the Tx to IRS link and the Tx to Rx link, respectively. Let $\mathbf{C}$ denote the spatial correlation matrix of IRS channel gains. With isotropic scattering the spatial correlation between IRS elements n and m with spacing d_{nm} is shown to be

$$[\mathbf{C}]_{n,m} = \text{sinc}\left(\frac{2d_{nm}}{\lambda}\right), \text{for } n,m=\{1,2,\ldots,N\}, \tag{23}$$

where $\text{sinc}(x) = \sin(\pi x)/(\pi x)$ [26]. Thus the channel gain matrix $\mathbf{G}$ and the channel gain vector $\mathbf{f}_m$ from the IRS to the m^{th} antenna of the Rx are given by

$$\mathbf{G} = \sqrt{\frac{K_g\mu_g}{K_g+1}}\mathbf{G}^{\text{LOS}} + \sqrt{\frac{\mu_g\mathbf{C}}{K_g+1}}\mathbf{G}^{\text{NLOS}}, \tag{24}$$

$$\mathbf{f}_m = \sqrt{\frac{K_r\mu_r}{K_r+1}}\mathbf{f}_m^{\text{LOS}} + \sqrt{\frac{\mu_r\mathbf{C}}{K_r+1}}\mathbf{f}_m^{\text{NLOS}}, \tag{25}$$

for $m\in\{1,2,\ldots,N_r\}$. Each element of the $\mathbf{G}^{\text{NLOS}}$ matrix and $\mathbf{f}_m^{\text{NLOS}}$ vector are distributed as i.i.d. $\mathcal{CN}(0,1)$. We consider independent Rayleigh fading for the direct link channel gain. Thus, $h_{mk}\sim\mathcal{CN}(0,\mu_d)$, where μ_d denotes the average channel power gain of the direct link.

A. Exact Analysis

Let $\mathbf{x}_{\text{opt}} = [x_{1,\text{opt}},\ldots,x_{N,\text{opt}}]$. Substituting optimal antenna indices $(s_{\text{opt}}, r_{\text{opt}})$, optimal reflection coefficient $x_{n,\text{opt}}$, and optimal power from Result 1 in (9), we get

$$\gamma = \frac{P_{\max}}{\sigma_n^2}\left(\underset{\substack{m\in\{1,2,\ldots,N_r\},\\ k\in\{1,2,\ldots,N_t\}}}{\max}\{Z_{mk}\}\right)^2, \tag{26}$$

where

$$Z_{mk} \triangleq |h_{mk}| + \sum_{n=1}^{N}|f_{mn}g_{nk}|. \tag{27}$$

Let $Z \triangleq \max_{m\in\{1,2,\ldots,N_r\},k\in\{1,2,\ldots,N_t\}}\{Z_{mk}\}$. From above, we see that the performance of the optimal rule depends on the statistics of the RV Z. Its CDF can be written as

$$F_Z(z) = \text{Pr}\left(\underset{m\in\{1,2,\ldots,N_r\},k\in\{1,2,\ldots,N_t\}}{\max}\{Z_{mk}\}\le z\right), \tag{28}$$

$$= \text{Pr}\left(Z_{11}\le z,\ldots,Z_{N_rN_t}\le z\right). \tag{29}$$

We note that the RVs $Z_{11}, Z_{21},\ldots,Z_{N_r1}$ are dependent as they are functions of $g_{11},\ldots,g_{N1}$. Similarly, $Z_{11}, Z_{12},\ldots,Z_{1N_t}$ are dependent. Therefore, $F_Z(z)$ involves order statistics of dependent RVs, which is in general hard to simplify.

We now provide two ways to evaluate $F_Z(z)$, first for general N_r and then for $N_r = 1$.

i) General N_r: Firstly, we condition on $\mathbf{f}_1,\ldots,\mathbf{f}_{N_r},\mathbf{G}$ and then average over them to get

$$F_Z(z) = \mathbb{E}\left[\text{Pr}\left(|h_{11}|+\sum_{n=1}^{N}|f_{1n}g_{n1}|\le z,\ldots \right.\right.$$
$$\left.\left.\ldots,|h_{N_rN_t}|+\sum_{n=1}^{N}|f_{N_rn}g_{nN_t}|\le z\,\middle|\,\mathbf{f}_1,\ldots,\mathbf{f}_{N_r},\mathbf{G}\right)\right]. \tag{30}$$

Given $\mathbf{f}_1, \ldots, \mathbf{f}_{N_r}$, and $\mathbf{G}$, the events $\left\{|h_{mk}| + \sum_{n=1}^{N} |f_{mn}|\,|g_{nk}| \leq z\right\}$, for $m \in \{1, 2, \ldots, N_r\}, k \in \{1, 2, \ldots, N_t\}$ are mutually independent as $h_{11}, \ldots, h_{N_r N_t}$ are independent RVs. Therefore, we get

$$F_Z(z) = \mathbb{E}\left[\prod_{m=1}^{N_r}\prod_{k=1}^{N_t} \Pr\left(Z_{mk} \leq z \,\middle|\, \mathbf{f}_m, g_{1k}, \ldots, g_{Nk}\right)\right], \tag{31}$$

Since, $|h_{mk}|$ is a Rayleigh RV, $F_Z(z)$ can be simplified as

$$F_Z(z) = \mathbb{E}\left[\prod_{m=1}^{N_r}\prod_{k=1}^{N_t}\left(1 - e^{-\frac{\left(z - \sum_{n=1}^{N}|f_{mn}g_{nk}|\right)^2}{\mu_d}}\right)\right], \tag{32}$$

if $z > \sum_{n=1}^{N} |f_{1n}g_{n1}|, \ldots, z > \sum_{n=1}^{N} |f_{N_r n}g_{nN_t}|$, otherwise $F_Z(z) = 0$. The expectation in (32) can be evaluated using Monte Carlo techniques.

ii) Special Case $N_r = 1$: We now present a simpler way to compute $F_Z(z)$ for $N_r = 1$. Here,

$$\begin{aligned} F_Z(z) =& \Pr\left(\max_{k\in\{1,2,\ldots,N_t\}}\{Z_{1k}\} \leq z\right), && (33)\\ =& \Pr\left(Z_{11} \leq z, \ldots, Z_{1N_t} \leq z\right), && (34)\\ =& \Pr\left(|h_{11}| + \sum_{n=1}^{N}|f_{1n}g_{n1}| \leq z, \ldots \right.\\ & \left. \ldots, |h_{1N_t}| + \sum_{n=1}^{N}|f_{1n}g_{nN_t}| \leq z\right). && (35)\end{aligned}$$

Conditioning on $\mathbf{f}_1$ and averaging over it, we get

$$\begin{aligned} F_Z(z) =& \mathbb{E}\left[\Pr\left(|h_{11}| + \sum_{n=1}^{N}|f_{1n}g_{n1}| \leq z, \ldots, \right.\right.\\ & \left.\left. \ldots, |h_{1N_t}| + \sum_{n=1}^{N}|f_{1n}g_{nN_t}| \leq z \,\middle|\, \mathbf{f}_1\right)\right]. \quad (36)\end{aligned}$$

Given $\mathbf{f}_1$, the events $\left\{|h_{1k}| + \sum_{n=1}^{N}|f_{1n}g_{nk}| \leq z\right\}$, for $k \in \{1, 2, \ldots, N_t\}$, are mutually independent. Furthermore, as the RVs are identically distributed, we get

$$\begin{aligned} F_Z(z) =& \mathbb{E}\left[\Pr\left(|h_{11}| + \sum_{n=1}^{N}|f_{1n}g_{n1}| \leq z \,\middle|\, \mathbf{f}_1\right)^{N_t}\right], && (37)\\ =& \mathbb{E}\left[\Pr\left(Z_{11} \leq z \,\middle|\, \mathbf{f}_1\right)^{N_t}\right]. && (38)\end{aligned}$$

It is difficult to obtain the CDF of Z_{11} given $\mathbf{f}_1$ as the RVs $g_{11}, \ldots, g_{N1}$ are correlated. Therefore, we use the moment matching method to match its distribution to a Gamma distribution with shape and scale parameters $\alpha(\mathbf{f}_1) = \left(\mathbb{E}\left[Z_{11}|\mathbf{f}_1\right]\right)^2/\mathrm{Var}\left[Z_{11}|\mathbf{f}_1\right]$ and $\beta(\mathbf{f}_1) = \mathbb{E}\left[Z_{11}|\mathbf{f}_1\right]/\mathrm{Var}\left[Z_{11}|\mathbf{f}_1\right]$. Therefore, $\Pr\left(Z_{11} \leq z \,\middle|\, \mathbf{f}_1\right) = \gamma\left(\alpha(\mathbf{f}_1), \beta(\mathbf{f}_1)\, z\right)/\Gamma(\alpha(\mathbf{f}_1))$, where $\gamma(\cdot,\cdot)$ is the lower incomplete gamma function and $\Gamma(\cdot)$ is gamma function [33]. Thus,

$$F_Z(z) = \mathbb{E}\left[\frac{\gamma\left(\alpha(\mathbf{f}_1), \beta(\mathbf{f}_1)\, z\right)}{\Gamma(\alpha(\mathbf{f}_1))}\right]. \tag{39}$$

We now express different performance metrics as a function of $F_Z(z)$.

1) *Average SNR $\left(\overline{SNR}\right)$:* Averaging (26), we get $\overline{\mathrm{SNR}} = P_{\max}\mathbb{E}\left[Z^2\right]/\sigma_n^2$. Expressing the second moment of the non-negative RV Z, i.e., $\mathbb{E}\left[Z^2\right] = \int_0^\infty z^2 f_Z(z)dz$, in terms of its CDF, we get

$$\overline{\mathrm{SNR}} = \frac{P_{\max}}{\sigma_n^2}\int_0^\infty \left(1 - F_Z\left(\sqrt{z}\right)\right) dz. \tag{40}$$

2) *Outage Probability:* Let P_{out} denote the probability that the instantaneous SNR γ in (26) is below a threshold γ_t, i.e., $\Pr(\gamma < \gamma_t)$. It is given by

$$P_{\text{out}} = \Pr\left(\left(P_{\max}Z^2/\sigma_n^2\right) \leq \gamma_t\right) = F_Z\left(\sqrt{\gamma_t\sigma_n^2/P_{\max}}\right). \tag{41}$$

3) *Ergodic Rate:* The ergodic rate, which we denote by $\overline{\mathsf{ER}}$, in terms of the CDF of instantaneous SNR γ can be written as $\overline{\mathsf{ER}} = \log_2 e \int_0^\infty \left(1 - F_\gamma(x)\right)/\left(1 + x\right) dx$ [27, (26)]. Expressing it in terms of the CDF of RV Z, we get exact expression for the ergodic rate as follows

$$\overline{\mathsf{ER}} = \log_2 e \int_0^\infty \left(1 - F_Z\left(\sqrt{x\sigma_n^2/P_{\max}}\right)\right)\frac{1}{1+x}dx. \tag{42}$$

4) *Average SEP $\left(\overline{\mathsf{SEP}}\right)$:* Substituting the instantaneous SNR of the optimal AS rule from (26) in the instantaneous SEP expression for M-ary phase shift keying (PSK) [34], we get

$$\mathsf{SEP}(\gamma) = \frac{1}{\pi}\int_0^{\left(1-\frac{1}{M}\right)\pi} \exp\left(-\frac{P_{\max}\sin^2\left(\frac{\pi}{M}\right)}{\sigma_n^2\sin^2(\theta)}Z^2\right)d\theta. \tag{43}$$

Averaging it over Z, yields

$$\begin{aligned}\overline{\mathsf{SEP}} =& \frac{1}{\pi}\int_0^{\left(1-\frac{1}{M}\right)\pi}\int_0^\infty \frac{P_{\max}\sin^2\left(\frac{\pi}{M}\right)}{\sigma_n^2\sin^2(\theta)} e^{-\frac{P_{\max}\sin^2\left(\frac{\pi}{M}\right)}{\sigma_n^2\sin^2(\theta)}z}\\ & \times F_Z\left(\sqrt{z}\right) dz\, d\theta. \quad (44)\end{aligned}$$

5) *Approximate SEP:* Substituting (26) in the approximate SEP expression in (4), yields $\mathsf{SEP}(\gamma) \approx c_1 \exp\left(-c_2 P_{\max}Z^2/\sigma_n^2\right)$, where c_1 and c_2 are modulation-dependent constants. It is a good approximation for Quadrature PSK, 8-PSK, and 16-QAM with $(c_1, c_2) = (0.5, 0.6)$, $(c_1, c_2) = (0.6, 0.18)$, and $(c_1, c_2) = (0.8, 0.12)$, respectively [25]. Furthermore, it is exact for differential Binary PSK with $(c_1, c_2) = (0.5, 1)$ and non-coherent binary frequency-shift-keying with $(c_1, c_2) = (0.5, 0.5)$ [27]. Averaging this approximate SEP, we get

$$\begin{aligned}\overline{\mathsf{SEP}} \approx& \frac{c_1 c_2 P_{\max}}{\sigma_n^2}\int_0^\infty e^{-\frac{c_2 P_{\max}}{\sigma_n^2}z} F_Z\left(\sqrt{z}\right) dz, && (45)\\ \approx& c_1\sum_{i=1}^{n} w_i F_Z\left(\sqrt{\frac{x_i\sigma_n^2}{c_2 P_{\max}}}\right), && (46)\end{aligned}$$

where x_i and w_i are the n abscissas and weights, respectively, for Gauss-Laguerre integration [35, pp. 923]. The above approximation applies to many constellations.

B. Asymptotic Analysis

We now derive closed-form expressions for large N.

1) Normalized Average SNR: Let $Y_{mk} = \sum_{n=1}^{N} |f_{mn} g_{nk}|$ and $\mu_y = \mathbb{E}[Y_{mk}]$. Therefore,

$$\mu_y = l_r \sum_{n=1}^{N} \sqrt{\mu_{r,n} \mu_{g,n}}, \tag{47}$$

where $\mu_{r,m} = \mu_r \sum_{m=1}^{N} \left| \left[\mathbf{C}^{1/2} \right]_{n,m} \right|^2$, $\mu_{g,m} = \mu_g \sum_{m=1}^{N} \left| \left[\mathbf{C}^{1/2} \right]_{n,m} \right|^2$, $l_r = \frac{\pi L_{1/2}(-K_r) L_{1/2}(-K_g)}{4\sqrt{(K_r+1)(K_g+1)}}$, and $L_{1/2}(\cdot)$ is the Laguerre polynomial of degree $1/2$ [33]. We know that f_{mn} and g_{nk} are independent with finite mean and bounded variance. Furthermore, from (23), we see that covariances of $h_{r,m}$ and $h_{r,n}$ and g_{mk} and g_{nk} tend to zero for $|m-n| \to \infty$. Under these conditions, with spatial correlation given in (23), for large N, it can be shown that [26, (21)]

$$\frac{1}{N} \sum_{n=1}^{N} |f_{mn} g_{nk}| \to l_r \sqrt{\mu_r \mu_g}. \tag{48}$$

Using (48), we derive the below result.

Result *2:* With spatial correlation of IRS channels, the normalized average SNR of the AS rule in Result 1, i.e.,

$$\frac{\overline{\mathsf{SNR}}}{N^2} \to \frac{P_{\max} \mu_d}{\sigma_n^2 N^2} \sum_{k=1}^{N_t N_r} \frac{1}{k} + \frac{P_{\max}}{\sigma_n^2} \mu_g \mu_r l_r^2 + \frac{P_{\max} l_r \sqrt{\mu_d \mu_g \mu_r \pi}}{\sigma_n^2 N} \sum_{k=1}^{N_t N_r} \binom{N_t N_r}{k} \frac{(-1)^{k+1}}{\sqrt{k}}. \tag{49}$$

Proof: The proof is given in Appendix B. ∎

Insights: The expression in (49) applies to any value of N_t, N_r and for a sufficiently large N. Among the three terms, the first term is the average SNR due to the direct link. It increases linearly as the direct link average channel power gain μ_d increases and logarithmically as the product $N_t N_r$ increases. The second term corresponds to the average SNR obtained through reflected link. It is proportional to the product $\mu_g \mu_r$ and is independent of N_t and N_r. The third term is the average SNR due to the coherent combination of the signal from the direct and the reflected links. It depends on $N_t N_r$ and the statistics of the direct and the reflected links. By multiplying (49) with N^2, we see that the first term, which is the average SNR due to the direct link, is independent of N. The second term, which is the average SNR due to the reflected link, grows as N^2 and the third term, which is the average SNR due to the combination of the direct link and the reflected link, grows linearly with N.

For large N, the normalized average SNR saturates to a constant independent of N as follows

$$\lim_{N \to \infty} \frac{\overline{\mathsf{SNR}}}{N^2} \to \frac{P_{\max}}{\sigma_n^2} \mu_r \mu_g \left(l_r \right)^2. \tag{50}$$

In Section VI, we will see that the value of N for which the normalized average SNR reaches this constant depends on distances between the Tx, IRS, and Rx.

2) Approximate Ergodic Rate: Using Jensen's inequality, we get the following upper bound $\overline{\mathsf{ER}} = \mathbb{E}[\log_2(1+\gamma)] \leq \log_2(1 + \mathbb{E}[\gamma]) = \log_2\left(1 + \overline{\mathsf{SNR}}\right)$, Multiplying (49) with N^2 and substituting it in the above bound yields the following closed-form approximation

$$\overline{\mathsf{ER}} \approx \log_2 \left(1 + \frac{P_{\max}}{\sigma_n^2} \left[\sum_{k=1}^{N_t N_r} \frac{\mu_d}{k} + N^2 \mu_g \mu_r l_r^2 + N l_r \sqrt{\mu_d \mu_g \mu_r \pi} \sum_{k=1}^{N_t N_r} \binom{N_t N_r}{k} \frac{(-1)^{k+1}}{\sqrt{k}} \right] \right). \tag{51}$$

From (51), we see that in the low SNR regime, the ergodic rate grows as $\mathcal{O}(N^2)$ and in the high SNR regime, it grows as $\mathcal{O}(\log_2(N))$. In Section VI, we shall see that it is tight.

3) Strong LOS: Under strong LOS conditions, i.e., $K_g \to \infty$ and $K_r \to \infty$, we know that $\sum_{n=1}^{N} |f_{mn} g_{nk}| / N = \sqrt{\mu_r \mu_g}$. Therefore, for strong LOS conditions, the above expressions will yield exact values by substituting $l_r = 1$.

V. Subset Antenna Selection

We now develop algorithms for subset AS ($N_{RF} > 1$) when Rx employs SC. Here, we first present a manifold optimization based subset selection (MOBSS) algorithm to solve $\mathcal{P}$. Then, we propose a simpler alternating optimization based subset selection (AOBSS) algorithm.

For a given Tx subset S, Rx antenna r, and passive beamforming vector $\mathbf{x}$, optimal transmit beamforming vector $\mathbf{w}_{\text{opt}}$ at the Tx is given by [18]

$$\mathbf{w}_{\text{opt}} = \sqrt{P_{\max}} \frac{\mathbf{h}_{rS}^{*} + \mathbf{G}_S^{\dagger} \mathbf{F}_r^{\dagger} \mathbf{x}^{*}}{\left\| \mathbf{h}_{rS}^{*} + \mathbf{G}_S^{\dagger} \mathbf{F}_r^{\dagger} \mathbf{x}^{*} \right\|}. \tag{52}$$

Substituting this in (2), we get $\mathsf{SNR}(S, \mathbf{w}, \mathbf{x}, r) = P_{\max} \left\| \mathbf{x}^{\mathrm{T}} \mathbf{F}_r \mathbf{G}_S + \mathbf{h}_{rS}^{\mathrm{T}} \right\|^2 / \sigma_n^2$. Thus, for a given S and r, we can find $\mathbf{x}$ that maximizes the signal power by solving:

$$\mathcal{P}_{rS}: \quad \max_{\mathbf{x}} \quad \left\| \mathbf{x}^{\mathrm{T}} \mathbf{F}_r \mathbf{G}_S + \mathbf{h}_{rS}^{\mathrm{T}} \right\|^2, \tag{53}$$

$$\text{s.t.} \quad |x_n| = 1, \quad n = 1, \ldots, N. \tag{54}$$

Similar to $\mathcal{P}_k$ in Section III-B, the objective function in $\mathcal{P}_{rS}$ is quadratic in $\mathbf{x}$ and is convex and the unit modulus constraint forms a complex circle manifold. Therefore, we propose a manifold optimization based subset AS algorithm below.

1) MOBSS Algorithm: Here, for each $S \in \mathcal{S}$ and $r \in \{1, 2, \ldots, N_r\}$, we solve $\mathcal{P}_{rS}$ using a conjugate gradient based manifold optimization technique [19]. We obtain a passive beamforming vector $\mathbf{x}_S$ that maximizes the signal power for S. This is repeated for all sets in $\mathcal{S}$. Then, the optimal subset S_{opt} is the one that yields maximum signal power and the optimal passive beamforming vector $\mathbf{x}_{\text{opt}} = \mathbf{x}_{S_{\text{opt}}}$. We then compute optimal transmit beamforming vector $\mathbf{w}_{\text{opt}}$ by substituting S_{opt} and $\mathbf{x}_{\text{opt}}$ in (52). These steps are illustrated in Algorithm 1.

Number of Pilot Transmissions Required and Computational Complexity: Here, the Tx has N_{RF} RF chains. Thus, we need $\lceil N_t / N_{RF} \rceil N_r$ number of pilots to estimate $N_t N_r$

Algorithm 1 Manifold Optimization Based Algorithm

1: Tx estimates N_tN_r direct link and N_tN_rN reflected link channel gains.
2: **for all** $S \in \mathcal{S}$ and $r \in \{1, 2, \ldots, N_r\}$ **do**
3: Obtain $\mathbf{x}_{rS}$ that solves $\mathcal{P}_{rS}$ using manifold optimization technique.
4: **end for**
5: $(r_{\text{opt}}, S_{\text{opt}}) = \underset{r\in\{1,2,\ldots,N_r\}, S\in\mathcal{S}}{\arg\max} \left\{ \left\| \mathbf{x}_{rS}^{\mathrm{T}} \mathbf{F}_r \mathbf{G}_S + \mathbf{h}_{rS}^{\mathrm{T}} \right\|^2 \right\}$.
6: $\mathbf{x}_{\text{opt}} = \mathbf{x}_{r_{\text{opt}} S_{\text{opt}}}$.
7: Compute $\mathbf{w}_{\text{opt}}$ by substituting S_{opt}, $\mathbf{x}_{\text{opt}}$, and r_{opt} in (52).
8: **return** $S_{\text{opt}}, \mathbf{w}_{\text{opt}}, \mathbf{x}_{\text{opt}}, r_{\text{opt}}$.

TABLE I
COMPLEXITY COMPARISON

AS rule	Computational complexity
Optimal AS for SC	$\mathcal{O}(N_tN_rN)$
LAS for SC	$\mathcal{O}(N_tN_r + N)$
Optimal AS for MRC	$\mathcal{O}(N_tN^{1.5})$
LAS for MRC	$\mathcal{O}(N_tN)$
MOBSS	$\mathcal{O}(N_r\,(N_t)^{N_{RF}}\,N^{1.5})$
AOBSS	$\mathcal{O}(N_rN_t \log(N_t) + NN_{RF})$
SDR [18]	$\mathcal{O}((N+1)^6)$

direct link channel gains and $\lceil N_t/N_{RF} \rceil N_rN$ pilots for the reflected link channel gains. MOBSS solves $\mathcal{P}_{rS}$ for each $r \in \{1, 2, \ldots, N_r\}$ and $S \in \mathcal{S}$, which means it solves $\mathcal{P}_{rS}$ for $\mathcal{O}(N_rN_t{}^{N_{RF}})$ times. Computational complexity for each $\mathcal{P}_{rS}$ is $\mathcal{O}(N^{1.5})$ [19]. Hence, the total computational complexity is $\mathcal{O}(N_rN_t{}^{N_{RF}}N^{1.5})$.

2) AOBSS Algorithm: For a given Rx antenna m, we first compute the selection metric used by the LAS rule, i.e., $|h_{mk}| + \left|\sum_{n=1}^{N} f_{mn}g_{nk}\right|$, for $k \in \{1, 2, \ldots, N_t\}$, and sort them in descending order. Then from the sorted list, it selects the first N_{RF} Tx antennas as the subset S_m corresponding to Rx antenna m. This procedure is repeated for all the Rx antennas and the subsets $S_1, \ldots, S_{N_r}$ are computed. It then selects the Rx antenna with highest direct link channel norm, i.e., $r = \arg\max_{m\in\{1,2,\ldots,N_r\}} \{\|\mathbf{h}_{mS_m}\|\}$, and then selects Tx subset $S = S_r$. We initialize $\mathbf{w} = \sqrt{P_{\max}}\mathbf{h}_{rS}/\|\mathbf{h}_{rS}\|$. Then, for (r, S), it solves for the transmit beamforming vector $\mathbf{w}_{r,S}$ and passive beamforming vector $\mathbf{x}_{r,S}$ iteratively.

For a given (r, S) and transmit beamforming vector $\mathbf{w}$, $\mathbf{h}_{rS}^{\mathrm{T}}\mathbf{w}$ is the effective channel gain from the Tx to Rx. Similarly, the n^{th} element of $\mathbf{F}_r\mathbf{G}_S\mathbf{w}$, i.e., $[\mathbf{F}_r\mathbf{G}_S\mathbf{w}]_n$ is the effective channel gain of the signal reflected through n^{th} IRS element. For these effective channel gains, from (11), the optimal passive beamforming reflection coefficient is given by

$$x_n = \exp\left(j \arg\left(\mathbf{h}_{rS}^{\mathrm{T}}\mathbf{w}\right) - j \arg\left([\mathbf{F}_r\mathbf{G}_S\mathbf{w}]_n\right)\right), \ \forall\ n. \quad (55)$$

The corresponding optimal $\mathbf{w}$ is obtained by substituting (55) in (52). We then update $\mathbf{x}$ by substituting the updated $\mathbf{w}$ in (55). This iterative process is continued till the SNR improvement is less than ϵ or the maximum number of iterations M is reached. Here, in each iteration, we alternatively optimize $\mathbf{x}$ for a given $\mathbf{w}$ and then optimize $\mathbf{w}$ given $\mathbf{x}$. These steps are illustrated in Algorithm 2.

TABLE II
PILOT TRANSMISSION COMPARISON

AS rule	Number of pilot transmissions
Optimal AS for SC	$N_tN_r + N_tN_rN$
LAS for SC	$2N_tN_r + N + 1$
Optimal AS for MRC	$N_tN_r + N_tN_rN$
LAS for MRC	$N_t + N_tN$
MOBSS	$\left\lceil \frac{N_t}{N_{RF}} \right\rceil N_r + \left\lceil \frac{N_t}{N_{RF}} \right\rceil N_rN$
AOBSS	$2\left\lceil \frac{N_t}{N_{RF}} \right\rceil N_r + N$
SDR [18]	$N + 1$

Number of Pilot Transmissions Required and Computational Complexity: Similar to MOBSS algorithm, we need $\lceil N_t/N_{RF} \rceil N_r$ pilots for the direct link CSI. However, for the reflected link CSI, we only need $\lceil N_t/N_{RF} \rceil N_r$ pilots to compute the selection metrics of the antennas and N pilots to compute the IRS reflection coefficients. This is because AOBSS algorithm uses the selection metric of the LAS rule. In total, we need $2\lceil N_t/N_{RF} \rceil N_r + N$ pilots. The number of computations required to select the subset is $\mathcal{O}(N_rN_t \log(N_t))$ and to compute $\mathbf{w}$ and $\mathbf{x}$ per iteration is $\mathcal{O}(NN_{RF})$. Unlike MOBSS, the computational complexity of AOBSS algorithm is independent of N_{RF} and the number of pilot transmissions required is also significantly lower. Table I compares the computational complexity and the Table II compares the number of pilot transmissions required for the proposed algorithms and SDR algorithm in [18].

Algorithm 2 Alternating Optimization Based Algorithm

1: For Rx antenna m, sort the selection metrics $|h_{mk}| + \left|\sum_{n=1}^{N} f_{mn}g_{nk}\right|$, for $k \in \{1, 2, \ldots, N_t\}$ in the descending order and assign indices of the first N_{RF} antennas to subset S_m.
2: Select $r = \arg\max_{m\in\{1,2,\ldots,N_r\}} \{\|\mathbf{h}_{mS_m}\|\}$ and $S = S_r$.
3: Estimate the reflected link CSI corresponding to (r, S).
4: **Initialize** $t = 0$, $\mathbf{w}^1 = \sqrt{P_{\max}}\mathbf{h}_{rS}/\|\mathbf{h}_{rS}\|$.
5: **while** (SNR improvement $> \epsilon$) and ($t \leq$ M) **do**
6: Update $t = t + 1$.
7: $x_n = \exp\left(j \arg\left(\mathbf{h}_{rS}^{\mathrm{T}}\mathbf{w}^t\right) - j \arg\left([\mathbf{F}_r\mathbf{G}_S\mathbf{w}^t]_n\right)\right)$.
8: $\mathbf{x}^t = [x_1, x_2, \ldots, x_N]$.
9: $\mathbf{w}^{t+1} = \sqrt{P_{\max}} \frac{\mathbf{h}_{rS}^* + \mathbf{G}_S^\dagger \mathbf{F}_r^\dagger (\mathbf{x}^t)^*}{\left\|\mathbf{h}_{rS}^* + \mathbf{G}_S^\dagger \mathbf{F}_r^\dagger (\mathbf{x}^t)^*\right\|}$.
10: **end while**
11: $\mathbf{w}_S = \mathbf{w}^{t+1}$.
12: $x_n = \exp\left(j \arg\left(\mathbf{h}_{rS}^{\mathrm{T}}\mathbf{w}_S\right) - j \arg\left([\mathbf{F}_r\mathbf{G}_S\mathbf{w}_S]_n\right)\right)$ and $\mathbf{x}_S = [x_1, x_2, \ldots, x_N]$
13: **return** S, $\mathbf{w}_S$, $\mathbf{x}_S$, and r.

Extension to Multiple Users: We note that our AS algorithms developed for a single user can be extended to many scenarios with multiple users. They can be employed in systems that employ time division multiple access and transmit to one user at a time. For example, systems that provide on demand video services by scheduling one user at a time. Furthermore, they can be used in WiFi systems that serve one user at a time or wireless power transfer systems that serve multiple sensor nodes based on a round robin scheduler.

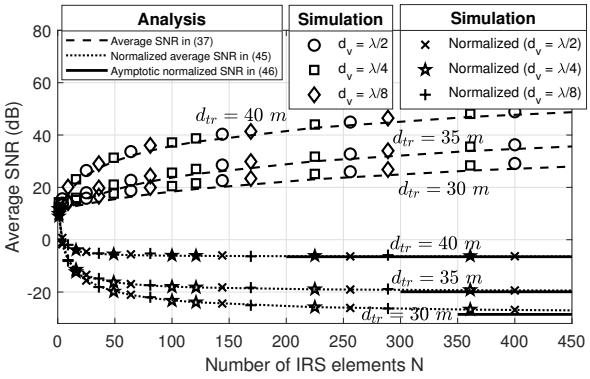

Fig. 3. Single AS: Average SNR of the optimal AS rule as a function of N when Rx is at different distances from the Tx and different values of IRS element spacing d_v ($N_t = 2$, $N_{RF} = 1$, $N_r = 2$, SC, $P_{\max} = 10$ dBm, and $d_{ti} = 40$ m).

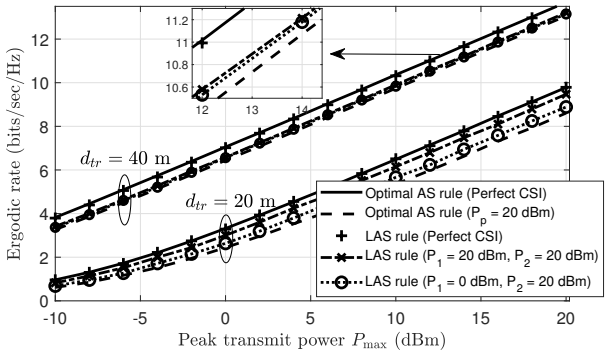

Fig. 4. Impact of imperfect CSI: Ergodic rate as a function of $P_{\max}$ for different distances ($N_{RF} = 1$, $N_t = 2$, $N_r = 2$, SC, $N = 49$, $d_v = \lambda/4$, $d_{ti} = 40$ m).

VI. Numerical Results

We will now study the performance of the proposed AS rules as a function of different system parameters. We consider a uniform linear array with half-wavelength antenna spacing at the Tx and a uniform planar array at the IRS. The Tx and IRS are placed such that there is a dominant LOS component between them. We set $K_g = 10$. We consider independent Rayleigh fading for the direct link from the Tx to the Rx, for the link from the IRS to the Rx ($K_r = 0$), and $\mathbf{G}_{\text{NLOS}}$. Furthermore, we consider correlated channel gains for Tx to IRS and IRS to Rx links. Correlation model in (23) is used. Our simulation setup is similar to [18]. The Tx and the IRS are located at a distance of d_{ti}. The Rx moves parallel to the line joining the Tx and IRS at a vertical distance of 2 m. Let d_{tr} and d_{ir} denote the distances from the Tx to Rx and IRS to Rx, respectively. The path-losses are taken to be $16.6{+}22\log_{10}(d_{ti})$, $35{+}30\log_{10}(d_{tr})$, and $20{+}30\log_{10}(d_{ir})$, respectively.[3] The noise variance σ_n^2 is set to -80 dBm. The SNR improvement threshold ϵ and a maximum number of iterations M are taken to be 10^{-4} and 5, respectively.

Single Antenna Selection: Figure 3 plots the average SNR and normalized average SNR of the optimal AS rule as a function of N with different IRS element spacing and for different values of d_{tr}. For a given d_{tr}, the average SNR increases as N increases. It increases faster as the Rx moves closer to the IRS as the reflected link gets stronger. As N increases, the normalized average SNR decreases for small values of N and reaches a floor equal to $P_{\max}\mu_g\mu_r l_r^2/\sigma_n^2$ for large N. It reaches this floor value for a smaller N as the Rx moves closer to the IRS. Also shown are the analytical expressions in (40), (49), and (50), which match well with the simulations. As discussed in Section IV, we see that the average SNR and normalized average SNR are independent of the channel correlation, which is a function of d_v.

[3]These are obtained for the simplified path-loss model with a signal attenuation of 30 dB at 1 m reference distance, a carrier frequency of 2.4 GHz, path-loss exponent of 2.2 for the link from the Tx to IRS, and a path-loss exponent of 3 for the remaining two links. Furthermore, antenna gains at the Tx, Rx, and IRS are taken to be 0 dB, 5 dB, 15 dB, respectively.

A. Impact of Imperfect CSI:

Figure 4 plots ergodic rate as a function of $P_{\max}$, It compares the performance of the optimal AS and LAS rules with perfect and imperfect CSI for Rx at two different distances. Minimum mean square error estimation is performed using the CSI acquisition procedure described in Section II-A for the optimal AS rule and using two pilot power procedure described in Section III-A3 for the LAS rule. With perfect CSI, the LAS rule performs similar to the optimal rule. With imperfect CSI, the performance of both rules degrade. However, degradation in the performance of the LAS rule is lower due to less number of channel estimations performed. Furthermore, the LAS rule performs better even with lower pilot power in the first phase, i.e., $P_1 = 0$ dBm. Thus, the LAS rule reduces the pilot power consumption significantly while being robust to estimation errors.

Figure 5 studies the impact of discrete phase shifts on the proposed single AS rules. Figures 5a and 5b plots ergodic rate as a function of $P_{\max}$ for SC and MRC, respectively. It increases as $P_{\max}$ increases. Furthermore, it also improves significantly as N increases. *i) SC:* We see that the ergodic rate with three bit quantized phase shift matches well with the ideal continuous phase shift. Therefore, a finite bit control link from Tx to IRS is sufficient. The performance of the proposed AS rule with one bit quantizer matches with that of the exhaustive search based AS rule that searches over all 2^N phase combinations. Thus, the proposed AS rules perform well with lower complexity. We also see that the approximate expression in (51) is close to the exact even for small $N = 36$ and matches for $N = 64$. System with $N = 64$ achieves the same rate as that of the $N = 16$ with 8 dBm lower transmit power. *ii) MRC:* Figure 5b compares the performance of manifold based AS rule with the LAS rule for MRC developed in Section III-B2. We see that the LAS rule is able to perform well even with 3 bit discrete phase levels.

Impact of Channel Correlation: Figure 6 plots outage probability as a function of $P_{\max}$. This is done for IRS element spacing $\lambda/2$ and $\lambda/4$ and different values of N_t, N_r, and N. Also shown are the analysis expressions using (32) and (39), which match well with the simulations. For a given $P_{\max}$, we see that the outage probability increases as

This article has been accepted for publication in IEEE Transactions on Wireless Communications. This is the author's version which has not been fully edited and content may change prior to final publication. Citation information: DOI 10.1109/TWC.2023.3235835

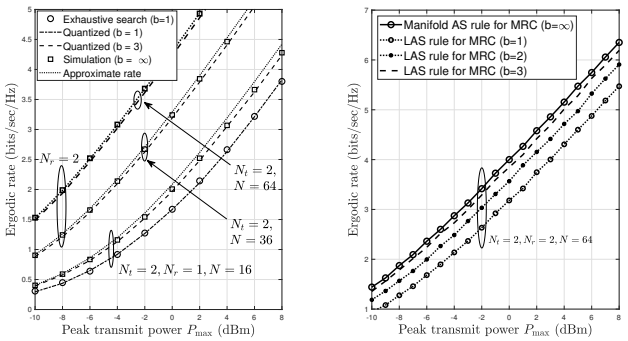

(a) SC (b) MRC

Fig. 5. Impact of discrete phase shifts: Ergodic rate as a function of $P_{\max}$ for different values of N_t, N_r, and N ($N_{RF} = 1$, $d_v = \lambda/8$, $d_{ti} = 40$ m, $d_{tr} = 35$ m).

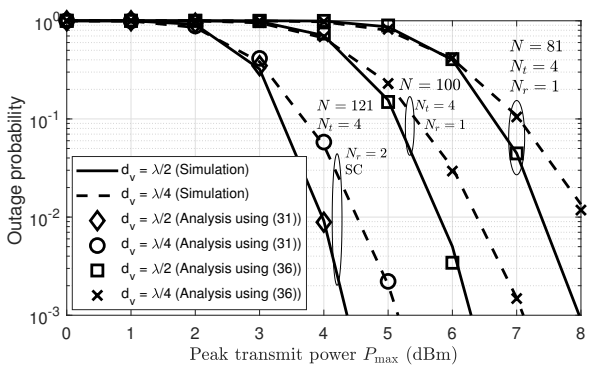

Fig. 6. Impact of channel correlation: Outage probability as a function of $P_{\max}$ for different IRS element spacing ($N_{RF} = 1$, $d_{ti} = 40$ m, $d_{tr} = 35$ m, $d_{ir} = 5.4$ m).

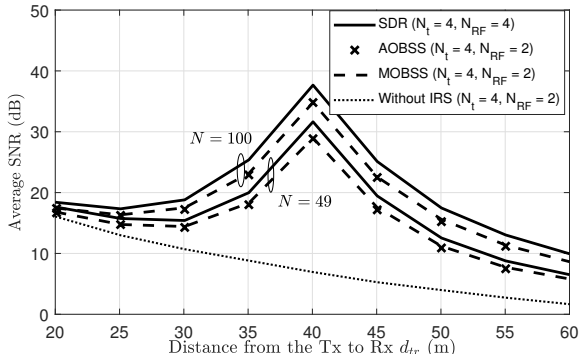

Fig. 7. Subset AS: The average SNR as a function of distance from the Tx to Rx for different values of N ($N_r = 1$, $P_{\max} = 5$ dBm, $d_v = \lambda/2$, and $d_{ti} = 40$ m).

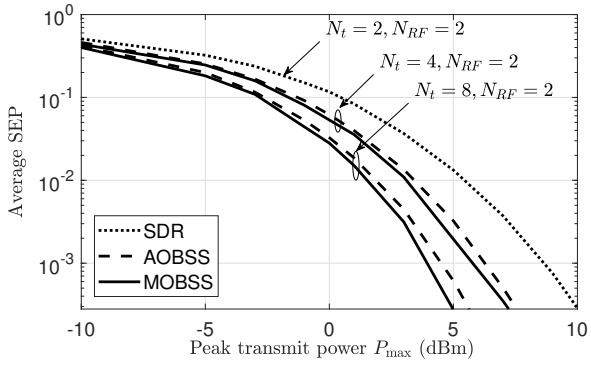

Fig. 8. Subset AS: Average SEP as a function of $P_{\max}$ for different number of antenna elements N_t ($N_r = 1$, $N = 10$, $d_v = \lambda/2$, $d_{ti} = 40$ m, $d_{tr} = 35$ m, $d_{ir} = 5.4$ m, and QPSK).

element spacing decreases. This is because the spatial channel correlation increases as the element spacing decreases. For $N = 100$, $N_t = 4$, and $N_r = 1$ at $P_{\max} = 6$ dBm outage probability with $d_v = \lambda/4$ is $6.4\times$ higher than that of the $d_v = \lambda/2$. Furthermore, at $P_{\max} = 6$ dBm, for $d_v = \lambda/2$, $N_t = 4$, and $N_r = 1$, the outage probability decreases by two orders of magnitude by increasing IRS elements from 81 to 100. Therefore, IRS-assisted AS improves the outage performance significantly even with channel correlation.

B. Subset Antenna Selection

Figure 7 plots the average SNR as a function of distance from Tx to Rx d_{tr}. It compares the performance of the proposed subset selection algorithms with the SDR-based beamforming technique that requires number of RF chains equal to the antennas [18]. Also, shown is the $\overline{\text{SNR}}$ when there is no IRS. It decreases as d_{tr} increases. With IRS, we see that the average SNR initially decreases as d_{tr} increases and then increases till $d_{tr} = 40$ m. This happens because the Rx moves closer to the IRS though it moves away from the Tx, which makes the reflected link stronger. Furthermore, the average SNR decreases for $d_{tr} > 40$ m as the Rx moves away from both the Tx and IRS. We see that an increase of 6 dB in SNR, which is maximum, occurs at $d_{tr} = 40$ m, i.e., when the Rx is close to the IRS. Note that the simpler AOBSS algorithm performs very close to the MOBSS algorithm. With SDR, which requires two additional RF chains, the SNR improvement is only 2.6 dB and 2.9 dB, for $N = 49$ and $N = 100$, respectively, at $d_{tr} = 40$ m. Therefore, the proposed subset selection algorithms perform well with less hardware.

Figure 8 plots the average SEP as a function of $P_{\max}$ for $N_{RF} = 2$ and different values of N_t with IRS channel correlation. It compares the performance of MOBSS and AOBSS algorithms. We see that the simpler AOBSS performs close to MOBSS. Also, shown is the performance of the SDR-based beamforming technique [18]. With a fixed number of RF chains, we see that the average SEP improves significantly by increasing the number of antenna elements. For example, at $P_{\max} = 5$ dBm, it reduces by a factor of 6.1 and 48.2 when $N_t = 4$ and $N_t = 8$, respectively compared to $N_t = 2$ with the same number of RF chains.

VII. Conclusions

We proposed algorithms that did joint AS, transmit beamforming at the Tx, and passive beamforming at the IRS. For single AS, we derived an optimal AS rules and also proposed a simpler yet near-optimal LAS rules. For SC, we showed that the optimal antenna depended only on the

absolute values of the channel gains and the optimal reflection coefficient depended only on their phases. Furthermore, they were decoupled. With IRS channel correlation, we derived exact expressions for the average SNR, outage-probability, ergodic rate, and average SEP of the optimal AS rule. From the closed-form expressions, we saw that the average SNR due to the reflected link grows quadratically and the average SNR due to the combination of the direct and reflected links grows linearly as the number of IRS elements increase. For MRC, we developed a manifold optimization based algorithm that converges to a local optimal solution and a LAS rule that requires lower number of pilots. For subset AS, we proposed MOBSS algorithm, whose subset search complexity is exponential in terms of number of RF chains, and AOBSS algorithm, whose subset search complexity is independent of the number of RF chains. Our results showed that for a fixed number of RF chains, the IRS-assisted AS system improved performance significantly even with imperfect CSI, discrete phase shifts, and channel correlation.

APPENDIX

A. Proof of Result 1

Here, to maximize the signal power at the Rx, the Tx transmits with power $P_{\max}$. Hence, from (8), the signal power is equal to $P_{\max}\left|h_{rs}+\sum_{n=1}^{N} f_{rn}g_{ns}x_n\right|^2$. Using triangle inequality, we know that

$$\left|h_{rs}+\sum_{n=1}^{N} f_{rn}g_{ns}x_n\right| \leq |h_{rs}|+\sum_{n=1}^{N}\left|f_{rn}g_{ns}x_n\right|, \tag{56}$$

where equality is achieved when $f_{rn}g_{ns}x_n, \forall\ n$, are phase aligned with the direct link channel h_{rs}, i.e., $\arg\left(f_{rn}g_{ns}x_n\right)=\arg\left(h_{rs}\right)$. Thus, for Tx antenna s and Rx antenna r, the maximum signal power is achieved when

$$\arg\left(x_n\right)=\arg\left(h_{rs}\right)-\arg\left(f_{rn}g_{ns}\right),\ \forall\ n, \tag{57}$$

which is equal to $P_{\max}\left(|h_{rs}|+\sum_{n=1}^{N}\left|f_{rn}g_{ns}\right|\right)^2$. Therefore, the optimal Tx antenna s_{opt} and Rx antenna r_{opt} are the ones that maximizes $|h_{rs}|+\sum_{n=1}^{N}\left|f_{rn}g_{ns}\right|$, for $r\in\{1,2,\ldots,N_r\}$ and $s\in\{1,2,\ldots,N_t\}$. They are given by (10). From (57), the corresponding optimal reflection coefficients are given by (11).

B. Proof of Result 2

The instantaneous SNR of the optimal AS rule normalized by N^2 is given by

$$\frac{\gamma}{N^2}=\frac{P_{\max}}{\sigma_n^2}\left(\max_{\substack{m\in\{1,2,\ldots,N_r\},\\ k\in\{1,2,\ldots,N_t\}}}\left\{\frac{|h_{mk}|}{N}+\sum_{n=1}^{N}\frac{|f_{mn}g_{nk}|}{N}\right\}\right)^2. \tag{58}$$

Substituting (48) in (58) and averaging yields

$$\frac{\overline{\text{SNR}}}{N^2}=\frac{P_{\max}}{\sigma_n^2}\mathbb{E}\left[\max_{m,k}\left\{\left(\frac{|h_{mk}|}{N}+l_r\sqrt{\mu_r\mu_g}\right)^2\right\}\right]. \tag{59}$$

Upon simplification, we get

$$\frac{\overline{\text{SNR}}}{N^2}=\frac{P_{\max}}{\sigma_n^2N^2}\mathbb{E}\left[\max_{m,k}\left\{|h_{mk}|^2\right\}\right]+\frac{P_{\max}}{\sigma_n^2}\mu_g\mu_r l_r^2 \tag{60}$$

$$+2\frac{P_{\max}}{\sigma_n^2N}l_r\sqrt{\mu_r\mu_g}\mathbb{E}\left[\max_{m,k}\left\{|h_{mk}|\right\}\right]. \tag{61}$$

Since $|h_{mk}|^2$ is an exponential RV, we know that $\mathbb{E}\left[\max_{m,k}\{|h_{mk}|^2\}\right]=\sum_{k=1}^{N_tN_r}(1/k)$ [36, (8)].

To simplify the expectation in the last term, we use the following result. For a non-negative RV A, we know that $\mathbb{E}[A]=\int_0^\infty \Pr(A>a)\,da$. Thus, we get

$$\mathbb{E}\left[\max_{m,k}\left\{|h_{mk}|\right\}\right]=\int_0^\infty\left(1-\left[\Pr\left(|h_{11}|\leq x\right)\right]^{N_rN_t}\right)dx, \tag{62}$$

where the second equality follows as the RVs $|h_{11}|,\ldots,|h_{N_rN_t}|$ are i.i.d. Substituting the CDF of Rayleigh RV $|h_{11}|$ and simplifying the integral, we get

$$\mathbb{E}\left[\max_{m,k}\left\{|h_{mk}|\right\}\right]=\sum_{k=1}^{N_rN_t}\binom{N_rN_t}{k}(-1)^{k+1}\frac{1}{2}\sqrt{\frac{\pi\mu_d}{k}}. \tag{63}$$

Substituting this along with $\mathbb{E}\left[\max_{m,k}\{|h_{mk}|^2\}\right]$ in (60) yields the expression for the normalized average SNR in (49).

REFERENCES

[1] R. Sarvendranath and A. K. R. Chavva, "Low-complexity joint antenna selection and beamforming for an IRS assisted system," in *Proc. WCNC*, Mar. 2021, pp. 1–6.

[2] J. Zhang, E. Björnson, M. Matthaiou, D. W. K. Ng, H. Yang, and D. J. Love, "Prospective multiple antenna technologies for beyond 5G," *IEEE J. Sel. Areas Commun.*, vol. 38, no. 8, pp. 1637–1660, Aug. 2020.

[3] Q. Wu and R. Zhang, "Towards smart and reconfigurable environment: Intelligent reflecting surface aided wireless network," *IEEE Commun. Mag.*, vol. 58, no. 1, pp. 106–112, Jan. 2020.

[4] N. B. Mehta, S. Kashyap, and A. F. Molisch, "Antenna selection in LTE: From motivation to specification," *IEEE Commun. Mag.*, vol. 50, no. 10, pp. 144–150, Oct. 2012.

[5] E. Basar, M. Di Renzo, J. De Rosny, M. Debbah, M. S. Alouini, and R. Zhang, "Wireless communications through reconfigurable intelligent surfaces," *IEEE Access*, vol. 7, pp. 116 753–116 773, Aug. 2019.

[6] I. Yildirim, A. Uyrus, and E. Basar, "Modeling and analysis of reconfigurable intelligent surfaces for indoor and outdoor applications in future wireless networks," *IEEE Trans. Commun.*, vol. 69, no. 2, pp. 1290–1301, Feb. 2021.

[7] A. Vaezi, A. Abdipour, A. Mohammadi, and F. Ghannouchi, "Analysis of nonlinear crosstalk impairment in MIMO-OFDM systems," *Analog Integrated Circuits and Signal Processing*, vol. 99, no. 3, pp. 559–569, Sep. 2018.

[8] H. Leung and Z. Zhu, *Signal Processing for RF Impairment Mitigation in Wireless Communications*. Artech, 2014. [Online]. Available: https://ieeexplore.ieee.org/document/9100474

[9] M. Jung, W. Saad, M. Debbah, and C. S. Hong, "On the optimality of reconfigurable intelligent surfaces (RISs): Passive beamforming, modulation, and resource allocation," *IEEE Trans. Wireless Commun.*, vol. 20, no. 7, pp. 4347–4363, Jul. 2021.

[10] D. Kudathanthirige, D. Gunasinghe, and G. Amarasuriya, "Performance analysis of intelligent reflective surfaces for wireless communication," in *Proc. ICC*, Jun. 2020, pp. 1–6.

[11] M.-A. Badiu and J. P. Coon, "Communication through a large reflecting surface with phase errors," *IEEE Wireless Commun. Lett.*, vol. 9, no. 2, pp. 184–188, Feb. 2020.

[12] D. L. Galappaththige, D. Kudathanthirige, and G. Amarasuriya, "Performance analysis of distributed intelligent reflective surface aided communications," in *Proc. Globecom*, Dec. 2020, pp. 1–6.

[13] S. Zhou, W. Xu, K. Wang, M. Di Renzo, and M.-S. Alouini, "Spectral and energy efficiency of IRS-assisted MISO communication with hardware impairments," *IEEE Wireless Commun. Lett.*, vol. 9, no. 9, pp. 1366–1369, Sep. 2020.

[14] N. K. Kundu and M. R. McKay, "RIS-assisted MISO communication: Optimal beamformers and performance analysis," in *Proc. Globecom*, Dec. 2020, pp. 1–6.

[15] Q. Wu and R. Zhang, "Intelligent reflecting surface enhanced wireless network via joint active and passive beamforming," *IEEE Trans. Wireless Commun.*, vol. 18, no. 11, pp. 5394–5409, Nov. 2019.

[16] P. Wang, J. Fang, X. Yuan, Z. Chen, and H. Li, "Intelligent reflecting surface-assisted millimeter wave communications: Joint active and passive precoding design," *IEEE Trans. Veh. Technol.*, vol. 69, no. 12, pp. 14 960–14 973, Dec. 2020.

[17] Y. Gao, C. Yong, Z. Xiong, D. Niyato, Y. Xiao, and J. Zhao, "Reconfigurable intelligent surface for MISO systems with proportional rate constraints," in *Proc. ICC*, Jun. 2020, pp. 1–7.

[18] Q. Wu and R. Zhang, "Intelligent reflecting surface enhanced wireless network: Joint active and passive beamforming design," in *Proc. Globecom*, Dec. 2018, pp. 1–6.

[19] X. Yu, D. Xu, and R. Schober, "MISO wireless communication systems via intelligent reflecting surfaces : (Invited Paper)," in *Proc. IEEE/CIC Int. Conf. Commun. China*, Aug. 2019, pp. 735–740.

[20] ——, "Optimal beamforming for MISO communications via intelligent reflecting surfaces," in *Proc. SPAWC*, May 2020, pp. 1–5.

[21] G. Zhou, C. Pan, H. Ren, K. Wang, and A. Nallanathan, "A framework of robust transmission design for IRS-aided MISO communications with imperfect cascaded channels," *IEEE Trans. Signal Process.*, vol. 68, pp. 5092–5106, Aug. 2020.

[22] C. Pan, H. Ren, K. Wang, W. Xu, M. Elkashlan, A. Nallanathan, and L. Hanzo, "Multicell MIMO communications relying on intelligent reflecting surfaces," *IEEE Trans. Wireless Commun.*, vol. 19, no. 8, pp. 5218–5233, Aug. 2020.

[23] C. Pan, H. Ren, K. Wang, M. Elkashlan, A. Nallanathan, J. Wang, and L. Hanzo, "Intelligent reflecting surface aided MIMO broadcasting for simultaneous wireless information and power transfer," *IEEE J. Sel. Areas Commun.*, vol. 38, no. 8, pp. 1719–1734, Aug. 2020.

[24] J. Ye, S. Guo, and M.-S. Alouini, "Joint reflecting and precoding designs for SER minimization in reconfigurable intelligent surfaces assisted MIMO systems," *IEEE Trans. Wireless Commun.*, vol. 19, no. 8, pp. 5561–5574, Aug. 2020.

[25] R. Sarvendranath and N. B. Mehta, "Impact of multiple primaries and partial CSI on transmit antenna selection for interference-outage constrained underlay CR," *IEEE Trans. Wireless Commun.*, vol. 18, no. 2, pp. 942–953, Feb. 2019.

[26] E. Björnson and L. Sanguinetti, "Rayleigh fading modeling and channel hardening for reconfigurable intelligent surfaces," *IEEE Wireless Commun. Lett.*, vol. 10, no. 4, pp. 830–834, Apr. 2021.

[27] F. A. Khan, K. Tourki, M. S. Alouini, and K. A. Qaraqe, "Performance analysis of a power limited spectrum sharing system with TAS/MRC," *IEEE Trans. Signal Process.*, vol. 62, no. 4, pp. 954–967, Feb. 2014.

[28] R. Sarvendranath and N. B. Mehta, "Antenna selection in interference-constrained underlay cognitive radios: SEP-optimal rule and performance benchmarking," *IEEE Trans. Commun.*, vol. 61, no. 2, pp. 496–506, Feb. 2013.

[29] D. Mishra and H. Johansson, "Channel estimation and low-complexity beamforming design for passive intelligent surface assisted MISO wireless energy transfer," in *Proc. ICASSP*, May 2019, pp. 4659–4663.

[30] B. Zheng and R. Zhang, "Intelligent reflecting surface-enhanced OFDM: Channel estimation and reflection optimization," *IEEE Wireless Commun. Lett.*, vol. 9, no. 4, pp. 518–522, Apr. 2020.

[31] S. T. Chung and A. J. Goldsmith, "Degrees of freedom in adaptive modulation: A unified view," *IEEE Trans. Commun.*, vol. 49, no. 9, pp. 1561–1571, Jan. 2001.

[32] P.-A. Absil, R. Mahony, and R. Sepulchre, *Optimization Algorithms on Matrix Manifolds*. Princeton University Press, 2008.

[33] L. S. Gradshteyn and L. M. Ryzhik, *Tables of Integrals, Series and Products*. Academic Press, 2000.

[34] M. Simon and M.-S. Alouini, *Digital Communication over Fading Channels*, 2nd ed. Wiley-Interscience, 2005.

[35] M. Abramowitz and I. Stegun, *Handbook of Mathematical Functions with Formulas, Graphs, and Mathematical Tables*, 9th ed. Dover, 1972.

[36] Ning Kong and L. B. Milstein, "Average SNR of a generalized diversity selection combining scheme," *IEEE Commun. Lett.*, vol. 3, no. 3, pp. 57–59, Mar. 1999.

Rimalapudi Sarvendranth (S'12-M'21) received his Bachelor of Technology degree in Electrical and Electronics Engineering from the National Institute of Technology Karnataka, Surathkal in 2009. He received his Master of Engineering and Ph.D. degrees from the Department of Electrical Communication Engineering, Indian Institute of Science, Bangalore in 2012 and 2020, respectively. He is currently working as an assistant professor in the Electronics and Electrical Engineering department of the Indian Institute of Technology Guwahati. In 2021, he was a postdoctoral researcher in the Department of Electrical Engineering, Linköping University, Sweden. From 2012 to 2016, he was with Broadcom Communications Technologies, Bangalore, India, where he worked on the development and implementation of algorithms for LTE and IEEE 802.11ac wireless standards. His research interests include machine learning for wireless communication, multiple antenna techniques, spectrum sharing, and next-generation wireless standards.

Ashok Kumar Reddy Chavva (Senior Member, IEEE) received his Bachelor of Technology degree in Electronics and Communications Engineering from the Jawaharlal Nehru Technological University, Hyderabad, India, in 2003, and the M.E. degree in telecommunication engineering from the Indian Institute of Science, Bangalore, India, in 2005. In June 2005, he joined Beceem Communications, which became part of Broadcom. Here, he was involved in developing physical layer algorithms for the first 4G system based on WiMAX and LTE. He worked with Broadcom till November 2013. Since November 2013, he has been with Samsung R & D Institute India Bangalore, India, where he currently leads an R & D team that works on 6G technologies. His research interests include algorithm design for the physical layer, performance evaluation of wireless communication systems, 5G/6G systems, X-MIMO, millimetre-wave and tera-hertz systems, and machine learning for communications. He received the best paper award at IEEE CCNC, Las Vegas, USA, 2016, the best paper (third) at IEEE World 5G Forum, 2020, and the winner of two challenges at ITU AI/ML 5G Challenge 2022.

Erik G. Larsson (Fellow) received the Ph.D. degree from Uppsala University, Uppsala, Sweden, in 2002. He is currently Professor of Communication Systems at Linköping University (LiU) in Linköping, Sweden. He was with the KTH Royal Institute of Technology in Stockholm, Sweden, the George Washington University, USA, the University of Florida, USA, and Ericsson Research, Sweden. His main professional interests are within the areas of wireless communications and signal processing. He co-authored *Space-Time Block Coding for Wireless Communications* (Cambridge University Press, 2003) and *Fundamentals of Massive MIMO* (Cambridge University Press, 2016).

He served as chair of the IEEE Signal Processing Society SPCOM technical committee (2015–2016), chair of the *IEEE Wireless Communications Letters* steering committee (2014–2015), member of the *IEEE Transactions on Wireless Communications* steering committee (2019-2022), General and Technical Chair of the Asilomar SSC conference (2015, 2012), technical co-chair of the IEEE Communication Theory Workshop (2019), and member of the IEEE Signal Processing Society Awards Board (2017–2019). He was Associate Editor for, among others, the *IEEE Transactions on Communications* (2010-2014), the *IEEE Transactions on Signal Processing* (2006-2010), and the *IEEE Signal Processing Magazine* (2018-2022).

He received the IEEE Signal Processing Magazine Best Column Award twice, in 2012 and 2014, the IEEE ComSoc Stephen O. Rice Prize in Communications Theory in 2015, the IEEE ComSoc Leonard G. Abraham Prize in 2017, the IEEE ComSoc Best Tutorial Paper Award in 2018, and the IEEE ComSoc Fred W. Ellersick Prize in 2019.